



## **An extracellular cell-attached pullulanase confers branched -glucan utilization in human gut *Lactobacillus acidophilus***

**Møller, Marie Sofie; Goh, Yong Jun; Rasmussen, Kasper Bøwig; Cypryk, Wojciech; Celebioglu, Hasan Ufuk; Klaenhammer, Todd R; Svensson, Birte; Abou Hachem, Maher**

*Published in:*  
Applied and Environmental Microbiology

*Link to article, DOI:*  
[10.1128/AEM.00402-17](https://doi.org/10.1128/AEM.00402-17)

*Publication date:*  
2017

*Document Version*  
Peer reviewed version

[Link back to DTU Orbit](#)

*Citation (APA):*  
Møller, M. S., Goh, Y. J., Rasmussen, K. B., Cypryk, W., Celebioglu, H. U., Klaenhammer, T. R., Svensson, B., & Abou Hachem, M. (2017). An extracellular cell-attached pullulanase confers branched -glucan utilization in human gut *Lactobacillus acidophilus*. *Applied and Environmental Microbiology*, 83(10), [AEM.00402-17]. <https://doi.org/10.1128/AEM.00402-17>

---

### **General rights**

Copyright and moral rights for the publications made accessible in the public portal are retained by the authors and/or other copyright owners and it is a condition of accessing publications that users recognise and abide by the legal requirements associated with these rights.

- Users may download and print one copy of any publication from the public portal for the purpose of private study or research.
- You may not further distribute the material or use it for any profit-making activity or commercial gain
- You may freely distribute the URL identifying the publication in the public portal

If you believe that this document breaches copyright please contact us providing details, and we will remove access to the work immediately and investigate your claim.

1 An extracellular cell-attached pullulanase confers branched  $\alpha$ -glucan utilization in human gut  
2 *Lactobacillus acidophilus*

3

4

5 Marie S. Møller,<sup>a</sup> Yong Jun Goh,<sup>b</sup> Kasper Bøwig Rasmussen,<sup>a</sup> Wojciech Cypryk,<sup>a</sup> Hasan Ufuk  
6 Celebioglu,<sup>a</sup> Todd R. Klaenhammer,<sup>b</sup> Birte Svensson,<sup>a</sup> Maher Abou Hachem<sup>a#</sup>

7

8 Department of Biotechnology and Biomedicine, Technical University of Denmark, Kgs. Lyngby,  
9 Denmark<sup>a</sup>; Department of Food, Bioprocessing and Nutrition Sciences, North Carolina State  
10 University, 7 Raleigh, North Carolina<sup>b</sup>

11

12 Running Head: Metabolism of branched  $\alpha$ -glucans by *L. acidophilus*

13

14 #Address correspondence to Maher Abou Hachem, [maha@bio.dtu.dk](mailto:maha@bio.dtu.dk) or Yong Jun Goh,  
15 [yjgoh@ncsu.edu](mailto:yjgoh@ncsu.edu).

## 16    **ABSTRACT**

17    Of the few predicted extracellular glycan-active enzymes, glycoside hydrolase family 13 subfamily  
18    14 (GH13\_14) pullulanases are the most common in human gut lactobacilli. These enzymes share a  
19    unique modular organization, not observed in other bacteria, featuring a catalytic module, two  
20    starch binding modules, a domain of unknown function, and a C-terminal surface layer association  
21    protein (SLAP) domain. Here we explore the specificity of a representative of this group of  
22    pullulanases, *LaPul13\_14* and its role in branched  $\alpha$ -glucans metabolism in the well characterized  
23    *Lactobacillus acidophilus* NCFM that is widely used as a probiotic. Growth experiments of *L.*  
24    *acidophilus* NCFM on starch-derived branched substrates revealed preference for  $\alpha$ -glucans with  
25    short branches of about two to three glucosyl moieties over amylopectin with longer branches. Cell-  
26    attached debranching activity was measurable in the presence of  $\alpha$ -glucans but was repressed by  
27    glucose. The debranching activity is conferred exclusively by *LaPul13\_14* and is abolished in a  
28    mutant strain lacking a functional *LaPul13\_14* gene. Hydrolysis kinetics of recombinant  
29    *LaPul13\_14* confirmed the preference for short branched  $\alpha$ -glucan oligomers consistent with the  
30    growth data. Curiously, this enzyme displayed the highest catalytic efficiency and the lowest  $K_m$   
31    reported for a pullulanase. Inhibition kinetics revealed mixed inhibition by  $\beta$ -cyclodextrin  
32    suggesting the presence of additional glucan binding sites besides the active site of the enzyme,  
33    which may contribute to the unprecedented substrate affinity. The enzyme also displays high  
34    thermostability and higher activity in the acidic pH range reflecting adaptation to the  
35    physiologically challenging conditions in the human gut.

## 36    **IMPORTANCE**

37    Starch is one of the most abundant glycans in human diet. Branched  $\alpha$ -1,6-glucans in dietary starch  
38    and glycogen are non-degradable by human enzymes and constitute a metabolic resource for the gut  
39    microbiota. The role of health-beneficial lactobacilli prevalent in the human small intestine in starch  
40    metabolism remains unexplored in contrast to colonic bacterial residents.

41 This study highlights the pivotal role of debranching enzymes in the break-down of starchy  
42 branched  $\alpha$ -glucan oligomers ( $\alpha$ -limit dextrins) by human gut lactobacilli exemplified by  
43 *Lactobacillus acidophilus* NCFM, which is one of the best characterized strains used as probiotics.

44 Our data bring novel insight into the metabolic preference of *L. acidophilus* for  $\alpha$ -glucans with  
45 short  $\alpha$ -1,6-branches. The unprecedented affinity of the debranching enzyme that confers growth on  
46 these substrates reflects its adaptation to the nutrient-competitive gut ecological niche and  
47 constitutes a potential advantage in cross-feeding from human and bacterial dietary starch  
48 metabolism.

## 49 INTRODUCTION

50 The human gastrointestinal tract is inhabited by a vast, diverse and dynamic microbial community  
51 (1), which is shaped by competition amongst the different taxa and selection by the host. *Firmicutes*  
52 and *Bacteroidetes* are the prevalent bacterial phyla of the human gut microbiota (HGM), followed  
53 by *Actinobacteria*, *Proteobacteria* and *Verrucomicrobia* in healthy adults (2). This microbial  
54 community provides protection against enteric pathogens and endows the host with metabolic  
55 activities that are not encoded in the human genome. More importantly, the interplay between diet  
56 and the HGM is currently recognized as a major effector of the composition of this community (2,  
57 3) and as a negotiator of human metabolism (4, 5). A key feature of the HGM is the ability to  
58 harvest energy from both host-derived and dietary glucans, particularly those resistant to digestion  
59 by human enzymes (6). Consequently differential glycan metabolism is a key affecter of the  
60 microbiota composition (7).

61 Starch is the most abundant glycan in human diet. This polysaccharide is a composite of two  $\alpha$ -  
62 glucans: the linear  $\alpha$ -1,4-glucan amylose, and amylopectin, which possesses approximately 5%  $\alpha$ -  
63 1,6-branch points with average branch lengths of 18–25 glucosyl moieties (8). Starch occurs  
64 naturally as supramolecular insoluble granules with semi-crystalline regions (8). These granules  
65 differ in size, structural properties as well as digestibility by bacterial and human enzymes. Humans  
66 digestive enzymes mainly target the  $\alpha$ -1,4-glucosidic bonds, but are less efficient in hydrolyzing  $\alpha$ -  
67 1,6-branches in starch (9). The digestibility of starch varies considerably based on botanical origin,  
68 crystal-packing and processing (10). Significant amounts of dietary starch escape digestion in the  
69 upper gastrointestinal tract (resistant starch, RS) (11) and are fermented in the colon by members of  
70 the gut microbiota (12–15). The small intestine, however, is dominated by bacteria from the Gram-  
71 positive *Lactobacillaceae* and the Gram-negative *Enterobacteriaceae* families (16). The former  
72 family contains human gut adapted lactobacilli from the *L. acidophilus* group, many strains of  
73 which are used as probiotics (17).

74 The ability of health beneficial bacteria from the *Lactobacillus* genus to grow on starch is limited  
75 to a handful of strains that grow on the soluble, but not granular starch (18, 19). Growth on short  
76 starch-derived malto-oligosaccharides ( $\alpha$ -gluco-oligosaccharides), however, is well established  
77 within this genus. Interestingly, a RS-rich diet appeared to boost the numbers of lactobacilli and  
78 lactate production in the distal colon in rodent models (20, 21). A recent human study in rural  
79 Malawi children showed a similar increase in lactobacilli after RS intake (22). A possible  
80 explanation of these observations is cross-feeding on short  $\alpha$ -glucans that are produced by primary  
81 starch degraders (14, 23). Cross-feeding requires efficient capture and transport systems and  
82 intracellular degrading enzymes reported to be conserved in this genus (24). The intracellular  $\alpha$ -  
83 glucoside utilization machinery of acidophilus group lactobacilli (17) is relatively well understood  
84 (24–26). By contrast, the extracellular  $\alpha$ -glucanolytic capabilities within this group of bacteria  
85 associated with a healthy gut microbiota are currently unexplored.

86 The commercial strain *Lactobacillus acidophilus* NCFM, which is used as probiotic, is among the  
87 best-studied of this taxonomic group (17). The genome of *L. acidophilus* NCFM (27) encodes nine  
88 enzymes of glycoside hydrolase family 13 (GH13), which harbors  $\alpha$ -glucan active enzymes  
89 according to the CAZy database (28). The only predicted  $\alpha$ -glucan active extracellular enzyme,  
90 however, is a pullulanase-type  $\alpha$ -glucan debranching enzyme. This enzyme is multi-modular  
91 comprising an N-terminal starch binding domain of carbohydrate binding module family 41  
92 (CBM41), followed by a domain of unknown function, a CBM48 domain, a GH13 subfamily 14  
93 (GH13\_14) catalytic module (28) and a C-terminal surface layer association protein (SLAP) (28,  
94 29) (Fig. 1). Pullulanases catalyze hydrolysis of  $\alpha$ -1,6-linked branches in glycogen, amylopectin  
95 and other starch derived glucans, as well as pullulan (Fig. 2) (30–32).

96 In this study, we show that extracellular cell-attached pullulanase activity can be measured upon  
97 growth of *L. acidophilus* NCFM on a range of oligomeric and polymeric  $\alpha$ -glucans, whereas this  
98 activity is repressed upon growth on glucose. We also establish the exclusive role of the  
99 debranching enzyme *LaPul13\_14* in the degradation of branched  $\alpha$ -glucans in this bacterium. The

100 catalytic and binding properties of the recombinant *LaPul13\_14* were investigated showing  
101 unprecedented substrate affinity and a clear preference towards short-branched  $\alpha$ -glucan oligomers  
102 as compared to amylopectin. These findings are consistent with the growth profile of *L. acidophilus*  
103 NCFM. Together, these findings highlight the role of *LaPul13\_14* and its homologues in mediating  
104 the utilization of branched oligomers derived from starch degradation in the human gut.

105

## 106 MATERIALS AND METHODS

107 **Materials.** High-purity (>95%) chemicals and commercial enzymes were from Sigma-Aldrich,  
108 MO, USA, unless otherwise stated. Pullulan (>95%) and  $\beta$ -limit dextrin (>97%) were from  
109 Megazyme (Bray, Ireland). The maltotetraose used for the growth/induction experiment was an in-  
110 house preparation (purity >92%; impurity was maltotriose). The branched  $\alpha$ -limit dextrin used for  
111 the kinetic analysis (kind gift from the late Bent S. Enevoldsen) comprises a mixture of two  
112 isomers: 6<sup>2</sup>- $\alpha$ -D-maltosyl-maltotriose and  $\alpha$ -D-glucosyl-maltotetraose.

113 **Bioinformatics analysis.** Sequences of *LaPul13\_14* homologues were extracted from the  
114 Carbohydrate-Active Enzymes database (CAZy; [www.cazy.org](http://www.cazy.org)) (28) using the CAZy tools  
115 provided by Alexander Holm Viborg (<http://research.ahv.dk>). Domain organisation of the protein  
116 sequences was analysed using a combination of batch searches in the Conserved Domain Database  
117 (29) and search in the Pfam protein families database (33). Identification of putative extracellular  
118 enzymes was done based on predictions from the SignalP 4.1 Server (34).

119 **Growth experiments.** *L. acidophilus* NCFM was grown on glucose, maltose, maltotriose,  
120 maltotetraose, a mixture of glucose and maltose (1:1 based on weight),  $\beta$ -limit dextrin,  
121 amylopectin or pullulan. Growth was performed in 14 ml semi-defined medium (SDM) (35) with  
122 0.5% (w/v) carbohydrate in 15 ml conical culture tubes, which were inoculated with an overnight  
123 culture previously grown on SDM supplemented with 1% (w/v) glucose to an optical density at 600  
124 nm ( $OD_{600}$ ) of 0.1 (0.04 as measured on 200  $\mu$ l culture in a 96-well plate using a microplate reader).  
125 The cultures were incubated at 37°C and 200  $\mu$ l samples were withdrawn every 1–2 hours for  $OD_{600}$

126 measurements. When the cultures reached late log-phase (after approx. 10 h),  $2 \times 1$  ml samples per  
127 culture were collected and spun down ( $20,000 \times g$ , 10 min,  $4^{\circ}\text{C}$ ) and the cells and supernatant were  
128 assayed for enzymatic activity (see below). The growth experiments of the *LaPul13\_14* deletion  
129 mutant ( $\Delta\text{LBA1710}$ , see below) were performed in a similar manner on glucose and maltose and all  
130 growth experiments were performed in duplicates. The supernatants from the growth experiments  
131 were assayed for pullulanase activity using the standard reducing sugar assay described below,  
132 whereas the cells were washed twice with 0.9% NaCl before measurements of pullulanase activity  
133 (described below).

134 Additional growth experiments were performed to compare the growth of *L. acidophilus* NCFM to  
135 *L. acidophilus* DSM-20242, which possesses identical organization of the maltodextrin utilization  
136 cluster as *L. acidophilus* NCFM and is used as a control, and *L. acidophilus* DSM-9126, which  
137 possesses a typical maltodextrin utilization locus and lacks the inserted transposase present in both  
138 *L. acidophilus* NCFM and DSM-20242. Anaerobically grown cultures in MRS were transferred  
139 once in SDM with 1% glucose (anaerobic), and the resulting cultures were used to inoculate (1% or  
140 equivalent cell density for weaker-growing strains) the SDM-based growth media (0.5%  
141 carbohydrate source, 200  $\mu\text{L}$  per well, in duplicate wells and conditions). Growth was monitored  
142 with a microtiter plate reader for 60 h.

143 **Maltooligosaccharide uptake.** *L. acidophilus* NCFM was grown on a total of 0.5% (w/v)  
144 mixture of maltose, maltotriose, and maltotetraose (1:1:1 based on weight) as described above.  
145 Samples were collected during growth for  $OD_{600}$  measurements and oligosaccharide analysis, which  
146 was performed as follows: 1 ml sample was spun down ( $20,000 \times g$ , 10 min,  $4^{\circ}\text{C}$ ), 80  $\mu\text{L}$   
147 supernatant was diluted 100-fold in 0.1 M NaOH and sterile filtered through pre-rinsed (with  
148 milliQ) 30 kDa filters (Amicon Ultra spin filters; Millipore, MA, USA) before the content of  
149 maltose, maltotriose and maltotetraose was analysed using high performance anion exchange  
150 chromatography with pulsed amperometric detection (HPAEC-PAD) using an ICS3000 system,  
151 equipped with CarboPac PA200 anion exchange column (Dionex Corporation, Sunnyvale, CA)



152 using a 2-step sodium acetate gradient (0–7 min: 37.5–75 mM and 7–30 min: 75–300 mM) and a  
153 constant concentration of 0.1 M NaOH at 25°C at 0.35 ml min<sup>-1</sup>. After each run the column was  
154 regenerated with a constant concentration of 0.1 M NaOH and 400 mM sodium acetate for 5 min,  
155 followed by a gradient from 400 mM to 37.5 mM sodium acetate over 5 min, and finally an  
156 equilibration with 37.5 mM sodium acetate and 0.1 M NaOH for 5 min.

157 **Construction of LBA1710 (*LaPul13\_14*) deletion mutant.** The 3,555-bp *lba1710* gene  
158 encoding the *LaPul13\_14* in *L. acidophilus* NCFM was deleted using a *upp*-based counterselective  
159 gene replacement system (36). Briefly, a 3,489-bp in-frame deletion (98% of gene) within *lba1710*  
160 was constructed by first PCR-amplifying the 629-bp and 646-bp DNA segments flanking the  
161 upstream and downstream of the *lba1710* deletion target, respectively, using primer pairs 1710-  
162 1/1710-2 (5'-GTAATAGGATCCACAACAAGCTCAAGGGATTCA-3' / 5'-  
163 AACACCTTTTGTTCCTTCCCA-3') and 1710-3/1710-4 (5'-  
164 TGGGGAACAAAAGGTGTTGCAGTGAATGTTGTTATTGAAG-3' / 5'-  
165 TTAGTAGAATTCCTTGAGGGAGCTCAACTTTC-3') (restriction sites were underlined), with  
166 PfuUltraII HS DNA Polymerase (Agilent Technologies, California, USA). Both purified PCR  
167 products were fused and amplified to generate copies of  $\Delta lba1710$  allele via splicing by overlap  
168 extension PCR (SOE-PCR) (37), using 10 ng of each PCR product as amplification templates in a  
169 50- $\mu$ L PCR reaction with primer pair 1710-1/1710-4 (see above). Purified SOE-PCR products  
170 (1,275 bp) were digested with BamHI and EcoRI and ligated into compatible ends of pTRK935  
171 counterselectable integration vector. Construction of the resulting recombinant integration plasmid  
172 containing the  $\Delta lba1710$  allele, designated pTRK1085, and the recovery of plasmid-free double  
173 recombinants with 5-fluorouracil were performed as described previously (36, 38). Double  
174 recombinants with  $\Delta lba1710$  allele were screened by colony PCR using primer pair 1710-1/1710-4.  
175 In-frame deletion and sequence integrity were confirmed by PCR and DNA sequencing using  
176 primer pair 1710-5/1710-6 (5'-TGAGCAAGTTAGCGCATCTG-3' / 5'-  
177 GCTGGTGTTCAGAAAGTAG-3'), which specifically anneal to the flanking region of the

178 *lba1710* gene. One of the confirmed  $\Delta lba1710$  deletion mutants, designated as NCK2325, was  
179 selected for further studies.

180 **Production and purification of recombinant LaPul13\_14.** *L. acidophilus* NCFM genomic  
181 DNA, prepared as previously described (26), was used to amplify the *LaPul13\_14* gene (locus tag  
182 number: LBA1710; GenBank accession number AAV43522.1), with the sense primer (5'-  
183 CTAGCTAGCGCAGAAACACCAGATGCTGG-3') and the antisense primer (5'-  
184 CCGCTCGAGAGCTTTTACTTCAATAACAACATTC-3') (restriction sites were underlined).  
185 The PCR amplicon encoding the mature peptide (3,468 bp) lacking the signal peptide (bp 1–105,  
186 corresponding to amino acid residues 1–35, see Fig. 1) was cloned within the *NheI* and *XhoI*  
187 restriction sites in pET21a(+) (Novagen, Darmstadt, Germany) and transformed into *Escherichia*  
188 *coli* XL10-Gold Ultra-competent cells (Stratagene, California, US) following the manufacturer's  
189 protocols. Transformants harboring pET21a(+)-*LaPul13\_14*, were selected on LB-agar plates with  
190 100  $\mu\text{g ml}^{-1}$  ampicillin and verified by restriction analysis and full sequencing. *E. coli* Rosetta  
191 (DE3) cells (Invitrogen, USA) transformed with pET21a(+)-*LaPul13\_14* were used for production  
192 of the enzyme.

193 The enzyme was produced in a 5-liter bioreactor (Biostat B Plus, Sartorius Stedium, Germany) as  
194 described elsewhere (39) with the following modifications: 3.7 liter defined medium was inoculated  
195 to  $OD_{600}=1.5$  with an overnight culture grown in LB medium. The fermentation was carried out at  
196 37°C until  $OD_{600}=8$ , before lowering the temperature to 15°C and induction of expression using 100  
197  $\mu\text{M}$  isopropyl- $\beta$ -D-thiogalactopyranoside. Cells were harvested ( $6,000 \times g$ , 20 min, 4°C) at  
198  $OD_{600}=30.5$  after 67 h of induction. The cell pellet was resuspended in buffer A (10 mM HEPES pH  
199 7.4, 25 mM imidazole, 40% glycerol, 0.5 M NaCl, 1 mM  $\text{CaCl}_2$ , 0.005 % (v/v) Triton X-100) and  
200 disrupted by high-pressure homogenization at 1000 bar. Disintegrated cells were treated with  
201 benzonase nuclease (Invitrogen; 30 min at room temperature) and centrifuged twice ( $40,000 \times g$ , 30  
202 min, 4°C). The supernatant was filtered (0.45  $\mu\text{m}$ ) and loaded onto a 5 ml HisTrap HP column (GE  
203 Healthcare, Uppsala, Sweden). After washing with 10 column volumes buffer A including 26 mM

imidazole, bound protein was eluted with a linear gradient from 3–80% buffer B (10 mM HEPES pH 7.4, 400 mM imidazole, 40% glycerol, 0.5 M NaCl, 1 mM CaCl<sub>2</sub>). Fractions containing protein were pooled and concentrated (30 kDa Amicon Ultra spin filters; Millipore) to 5 ml and loaded onto a pre-equilibrated HiLoad 26/60 Superdex G200 column (GE Healthcare) and eluted with 50 mM MES, pH 6.0, 1 mM CaCl<sub>2</sub>, 20% glycerol, 150 mM NaCl at 0.75 ml min<sup>-1</sup>. Fractions containing *LaPul13\_14* were pooled and desalted on a HiPrep 26/10 Desalting column (GE Healthcare) against 1 mM HEPES, pH 7.0. Desalted protein fractions were pooled and loaded onto a Resource Q column (6 ml; GE Healthcare) equilibrated with 10 mM HEPES, pH 7.0, at a flow rate of 2 ml min<sup>-1</sup>. Protein was eluted by a linear gradient (from 0–100% in 30 column volumes) of 10 mM HEPES, pH 7.0, 0.5 M NaCl. Fractions containing *LaPul13\_14* were pooled, concentrated, and buffer exchanged (30 kD Amicon Ultra spin filters, Millipore) to 50 mM MES pH 6.0, 20% glycerol, 0.5 mM CaCl<sub>2</sub>, 150 mM NaCl. The concentration of *LaPul13\_14* (SDS-PAGE) was determined spectrophotometrically using a molar extinction coefficient  $\epsilon_{280}=179,566 \text{ M}^{-1}\text{cm}^{-1}$  as determined by amino acid analysis (40).

**Enzyme activity assays and kinetics.** Determination of specific activity as well as kinetic parameters of *LaPul13\_14* was performed using a reducing sugar assay as previously described (41). In short; 1.1 ml reactions containing substrate (0.225 mg ml<sup>-1</sup> pullulan for specific activity; 0.02–1 mg ml<sup>-1</sup> pullulan, 0.1–10 mg ml<sup>-1</sup> potato amylopectin dissolved in 8 % (v/v) DMSO or 0.225–9 mg ml<sup>-1</sup>  $\beta$ -limit dextrin for kinetic analysis) and *LaPul13\_14* (0.05–1.5 nM) in assay buffer (20 mM sodium acetate pH 5.0, 5 mM CaCl<sub>2</sub>, 0.005% TritonX-100) were incubated at 37 °C and aliquots (200  $\mu$ l for pullulan, and 100  $\mu$ l for amylopectin and  $\beta$ -limit dextrin) were removed at five time points (3, 6, 9, 12, and 15 min) and added to 500  $\mu$ l stop solutions (0.4 M sodium carbonate pH 10.7, 2.5 mM CuSO<sub>4</sub>, 2.5 mM 4,4'-dicarboxy-1,2'-biquinoline, 6 mM L-serine). Milli-Q water was added to a final volume of 1 ml and  $A_{540\text{nm}}$  was measured after 30 min incubation at 80°C. The release of reducing sugars was quantified using a maltose standard. One activity unit (U) is defined as the amount of enzyme that releases one micromole of maltose reducing-sugar equivalents per

230 min from pullulan under assay conditions. The kinetic parameters  $K_m$  and  $k_{cat}$ , were determined by  
231 fitting the Michaelis-Menten equation to the initial velocity data. The data obtained were analyzed  
232 using the Enzyme Kinetics Module 1.0 of the program Sigmaplot 9.01 (Systat Software, Chicago,  
233 IL). Inhibition kinetics of *LaPul13\_14* by  $\beta$ -cyclodextrin ( $\beta$ -CD) were investigated using pullulan as  
234 substrate. The kinetics assay was done as described above, but with 50  $\mu$ M  $\beta$ -CD included. The data  
235 obtained was analyzed by fitting competitive, non-competitive, mixed inhibition models to the data  
236 using the Enzyme Kinetics Module 1.0 of the program Sigmaplot 9.01 (Systat Software, Chicago,  
237 IL), and the inhibition kinetics models were ranked based on  $\chi^2$  of the fits.

238 The hydrolysis kinetics parameters of the branched  $\alpha$ -limit dextrin mixture described above (five  
239 glucose units, maltosyl branch) by *LaPul13\_14* were determined using HPAEC-PAD. The starting  
240 reaction volume was 300  $\mu$ l including branched substrate (0.0625–1 mM) and 0.53 nM *LaPul13\_14*  
241 in 20 mM sodium acetate pH 5.0, 5 mM  $\text{CaCl}_2$ , 0.005% (v/v) TritonX-100. At four time points (3,  
242 6, 9, and 12 min) 60  $\mu$ l aliquots were drawn and mixed with 15  $\mu$ l 0.5 M NaOH. The samples were  
243 spun (20,000  $\times$  g, 5 min, 4°C) before 65  $\mu$ l samples were mixed with 65  $\mu$ l 0.1 M NaOH. The  
244 products were quantified based on peak areas from HPAEC-PAD analysis, which was performed as  
245 described above.

246 The described standard reducing sugar assay was also used to determine the pullulanase activity  
247 in the *L. acidophilus* culture supernatant and in the washed cell pellets, with the following  
248 exceptions: cells from 1 ml culture in the late log phase (see above) were resuspended in 600  $\mu$ l  
249 preheated (37°C) pullulan solution (0.4 mg ml<sup>-1</sup> pullulan, 40 mM sodium acetate pH 5.0, 0.5 mM  
250  $\text{CaCl}_2$ , 0.005% (v/v) Triton X-100), while 100  $\mu$ l culture supernatant was mixed with 500  $\mu$ l 0.48  
251 mg ml<sup>-1</sup> pullulan solution. Aliquots (100  $\mu$ l) were drawn after 0, 1, 2, and 3 h. The samples were  
252 spun down at 4°C for 2 min, and 75  $\mu$ l cell free sample was mixed with 500  $\mu$ l stop solution (0.4 M  
253 sodium carbonate pH 10.7, 2.5 mM  $\text{CuSO}_4$ , 2.5 mM 4,4'-dicarboxy-1,2'-biquinoline, 6 mM L-  
254 serine) and 425  $\mu$ l milliQ water. As a control, the degradation products from the assay with whole  
255 cells and pullulan were analyzed using thin layer chromatography (TLC). Samples (6  $\mu$ l) were

256 drawn after 0 and 19 h of reaction and spotted directly onto a TLC Silica 60 F<sub>254</sub> plate (Merck,  
257 Darmstadt, Germany), developed by isopropanol/ethyl acetate/water (60:20:20, v/v) and sprayed  
258 with 2% (w/v) orcinol in ethanol/H<sub>2</sub>SO<sub>4</sub>/water (80:10:10) followed by tarring at 300°C. The  
259 following standards were included on the gel (1 µl): 20 mM of either glucose, maltose, maltotriose  
260 and panose in water.

261 **Temperature and pH activity profiles.** The reducing sugar assay described above was used for  
262 determining the dependence of initial reaction rates on temperature in the range 7–80°C using 0.46  
263 nM *LaPul13\_14* and 0.225 mg ml<sup>-1</sup> pullulan. The dependence of activity on pH in the range 2.0–8.5  
264 was assayed using the reducing sugar assay described above in 20 mM of either glycine (pH 2.0–  
265 3.5), sodium acetate (pH 3.5–5.5), MES (pH 5.5–7.0), or HEPES (7.0–8.5) all including 0.5 mM  
266 CaCl<sub>2</sub> and 0.005% bovine serum albumin.

267 **Surface plasmon resonance (SPR) binding analysis of cyclodextrins.** The affinity of  
268 *LaPul13\_14* towards α-, β-, and γ-CD was analyzed using SPR on a BIAcore T100 (GE  
269 Healthcare). Random amine coupling was used to immobilize the enzyme on a CM5 sensor  
270 according to the manufacturer's protocol using 100 µg ml<sup>-1</sup> protein in 10 mM sodium acetate, pH 4,  
271 0.5 mM CaCl<sub>2</sub>, and 1 mM β-CD to a final chip density of 5477 response units (RU). The analysis  
272 comprised 100 s and 90 s for the association and dissociation phases, respectively, at a flow rate of  
273 30 µl min<sup>-1</sup> and 25°C at 19 β-CD concentrations (0.25–1024 µM) as well as 18 α-CD and γ-CD  
274 concentrations (3–5000 µM) all in 10 mM sodium acetate, pH 5.0, 150 mM NaCl, 0.005% (v/v)  
275 P20 surfactant. In the case of β-CD the interaction was analysed at 15°C and 37°C in addition to the  
276 25°C standard analysis. Furthermore, the interaction with β-CD was also analyzed at pH 7.0 in 10  
277 mM HEPES, pH 7.0, 150 mM NaCl, 0.005% P20 surfactant. A one site binding model was fit to the  
278 steady-state response blank and reference cell corrected sensorgrams using the BIA evaluation  
279 software supplied with the instrument.

280 **Starch binding assay.** Barley starch was washed three times in water followed by one time in  
281 assay buffer (40 mM sodium acetate pH 5.0, 0.5 mM CaCl<sub>2</sub>, 0.005% (v/v) Triton X-100) overnight.

282 Fifty microliters of *LaPul13\_14* diluted to 40 nM in assay buffer and 450  $\mu$ l of washed starch  
283 suspension in reaction buffer (25, 50, 100, 200 mg ml<sup>-1</sup>) were mixed and shaken vigorously at 4°C  
284 for 30 min. The mixture was subsequently centrifuged (20,000  $\times$  g, 5 min, 4°C) and 110  $\mu$ l of  
285 supernatant were used for the standard reducing sugar assay described above using 0.72 mg ml<sup>-1</sup>  
286 pullulan in assay buffer as substrate. Samples were withdrawn at 0 and 10 min and directly  
287 transferred to stop solution and the standard assay protocol was followed. The fraction of enzyme  
288 bound to starch was determined based on the activity in the supernatant relative to an enzyme  
289 sample without starch included.

290

## 291 RESULTS

292 ***L. acidophilus* growth on  $\alpha$ -glucans and extracellular pullulanase activity.** To assess the  $\alpha$ -  
293 glucan metabolic capabilities of *L. acidophilus* NCFM, growth was performed on glucose,  $\alpha$ -1,4-  
294 linked maltooligosaccharides with degree of polymerization (DP) of 2–4, amylopectin,  $\beta$ -limit  
295 dextrin possessing short branches (degradation product from hydrolysis of amylopectin by  $\beta$ -  
296 amylase) and pullulan (Fig. 2). *L. acidophilus* NCFM clearly preferred glucose followed by  
297 maltose, whereas the growth on the larger malto-oligosaccharides was much weaker (Fig. 3A).  
298 Amongst the branched polymeric  $\alpha$ -glucans, only  $\beta$ -limit dextrin with the short branches (mainly  
299 maltosyl) seemed to sustain clear, albeit low, growth (Fig. 3A), whereas no significant growth was  
300 observed on pullulan and amylopectin (data not shown). Cells harvested in the late log phase  
301 displayed highest cell-associated pullulanase activity when maltose was used as a carbon source,  
302 but maltotriose, maltotetraose and  $\beta$ -limit dextrin also resulted in a significant pullulanase activity  
303 (Fig. 3B). By contrast no significant activity was detected when the cells were grown on either  
304 glucose or a glucose:maltose 1:1 mixture. No pullulanase activity was detected in the culture  
305 supernatant, *i.e.* all pullulanase activity measured is entirely associated with the cells.

306 The uptake preference of maltooligosaccharides with degree of polymerization 2–4 by *L.*  
307 *acidophilus* NCFM was analyzed using a mixture of maltose, maltotriose, and maltotetraose as

308 carbohydrate source and the depletion of these saccharides in culture supernatants was monitored.  
309 Maltose was clearly the preferred substrate, but both maltotriose and maltotetraose were also taken  
310 up, albeit at a considerably slower rate (Fig. 3C).

311 To verify that the measured cell-associated pullulan hydrolyzing activity stems from *LaPul13\_14*,  
312 the gene encoding this enzyme was deleted and the *L. acidophilus* NCFM gene KO strain was  
313 grown on glucose or maltose. No cell-associated pullulanase activity was measured from this strain,  
314 although the growth rate on maltose was much higher as compared with wildtype (Fig. 4).

315 **Enzymatic properties of *LaPul13\_14*.** *LaPul13\_14* was produced recombinantly in *E. coli* and  
316 purified (yield 0.26 mg g<sup>-1</sup> cell wet weight) and migrated according to the predicted molecular mass  
317 of 129.4 kDa. The enzyme displayed a very high specific activity of 611 U mg<sup>-1</sup> toward pullulan  
318 corroborating the predicted specificity. The highest specific activity was measured at pH 5.0, and  
319 the enzyme retained more than 50% of its maximum activity in the pH range 2.5–6.5. The highest  
320 activity was measured at 55°C (at pH 5.0) and the Arrhenius activation energy was determined to  
321 60.2 kJ mol<sup>-1</sup>.

322 **Kinetic analysis.** The kinetic analysis performed on pullulan showed an exceptionally high  
323 catalytic efficiency ( $k_{\text{cat}}/K_m$ ) of 10368 ml s<sup>-1</sup>mg<sup>-1</sup> owing to a combination of a very low  $K_m$  value  
324 (0.05 mg ml<sup>-1</sup>) and a high catalytic turnover number ( $k_{\text{cat}}$ , 518 s<sup>-1</sup>) (T). Among the branched  
325 substrates tested, the catalytic efficiency decreased with increasing substrate size and branch length.  
326 Thus, the catalytic efficiency on the branched substrate  $\beta$ -limit dextrin, which has mainly maltosyl  
327 branches, was 14-fold higher than the corresponding value on amylopectin.

328 Cyclodextrins are well-known starch mimic molecules that bind tightly in the active sites of  
329 pullulanases resulting in apparent competitive inhibition (41). Interaction of  $\alpha$ -,  $\beta$ -, and  $\gamma$ -CD with  
330 *LaPul13\_14* was determined by SPR analysis.  $\beta$ - and  $\gamma$ -CD had dissociation constants ( $K_D$ ) of 10.8  
331 and 11.2  $\mu$ M, respectively (

TABLE 1. Binding of cyclodextrins to *LaPul13\_14* determined  
by surface plasmon resonance.

332 ). Interestingly, enzymatic inhibition kinetics analysis with pullulan revealed that the inhibition of  
333 *LaPul13\_14* with  $\beta$ -CD was not pure competitive inhibition, but was mixed type inhibition giving a  
334  $K_i$  of 35.9  $\mu$ M. This is an average value of the binding to the active site and possibly other binding  
335 site of lower affinity. The analysis of the binding of the enzyme to granular starch revealed only  
336 very low binding affinity hampering a reliable quantitative measurement (Fig. S1).

337

## 338 DISCUSSION

339 *Surface layer association proteins mediate attachment of glycan active enzymes and other*  
340 *functionally important enzymes to the cell envelope in Lactobacillus. L. acidophilus* NCFM is one  
341 of the most well-studied gut bacteria, which is ascribed health benefits and used as a commercial  
342 probiotic (42–45). The commercial and physiological relevance of *L. acidophilus* NCFM has  
343 spurred wide interest in the saccharide uptake and catabolism machinery of this organism to identify  
344 efficiently utilized glycans with potential as prebiotics (25, 46, 47). A few intracellular carbohydrate  
345 active enzymes (CAZymes) from *L. acidophilus* NCFM have been characterized including those  
346 active on maltose (26) and  $\alpha$ -1,6-linked isomaltooligosaccharides (24). However, insight is scarce  
347 into the extracellular CAZymes encoded by this bacterium and related human gut adapted  
348 lactobacilli (27). Recently, the first extracellular glycoside hydrolase from *L. acidophilus* NCFM  
349 was shown to be a  $\beta$ -N-acetylglucosaminidase autolysin essential for cell division (48). This  
350 enzyme harbors a surface layer association protein (SLAP) domain (Pfam family PF03217 (33))  
351 that confers noncovalent attachment to the proteinaceous outermost surface layer common in  
352 several lactobacilli (49). SLAP domains also occur at the C-termini of other functionally important  
353 proteins such as autolysins, fibronectin and mucin binding proteins, putative peptidases, nucleases,  
354 glycoside hydrolases as well as polysaccharides lyases according to the Pfam database (33). This  
355 suggests that SLAP domains constitute a general cell attachment scaffold that is fused to a select set



356 of activities destined for cell-surface display. The prevalence of this domain in the S-layer  
357 exoproteome of distinct lactobacilli is also in agreement with this role (50).

358 In this study, we present the functional characterisation of the SLAP domain-containing enzyme  
359 from *L. acidophilus* NCFM that is active on starch derived dietary glucans.

360 ***LaPul13\_14 is a cell-attached debranching enzyme that exclusively confers the utilization of***  
361 ***branched  $\alpha$ -glucans in *L. acidophilus*.*** Growth experiments of *L. acidophilus* NCFM clearly  
362 showed a preference for glucose and maltose as substrates. Low levels of growth was observed on  
363 the longer  $\alpha$ -1,4-maltooligosaccharides maltotriose and maltotetraose, and on  $\beta$ -limit dextrin, which  
364 is a model substrate that contains only short  $\alpha$ -1,6-branches (shown experimentally to be main 2–3  
365 glucosyl units for the substrate used in the present study, Fig. 2). By contrast, very little or no  
366 growth was observed on pullulan and amylopectin that contains longer branches (data not shown).  
367 Since *L. acidophilus* NCFM is only able to use the debranched maltose from  $\beta$ -limit dextrin, the  
368 energy yield per mass of this substrate is much lower compared to growth on maltose. Therefore,  
369 the observed low level of growth on  $\beta$ -limit dextrin is in agreement with the debranching activity of  
370 the cells and the lack of  $\alpha$ -amylase activity that is required for the full-utilization of this substrate.  
371 The poor growth on maltotriose and maltotetraose is, however, surprising as these substrates are  
372 predicted to be internalized through a maltodextrin specific ATP-binding cassette (ABC) system  
373 (LBA1864–LBA1867), which is conserved in acidophilus group lactobacilli (24). The  
374 corresponding transporter from the taxonomically related Gram-positive pathogen *Streptococcus*  
375 *pneumoniae* mediates the uptake of maltooligosaccharides up to eight units with a preference to  
376 maltotetraose (51). The expression of the ABC uptake system may be affected by an inserted  
377 transposase (LBA1868) that separates the catabolic genes from the transporter in *L. acidophilus*  
378 NCFM, but not in other lactobacilli (24). Nonetheless, the maltooligosaccharide uptake profile  
379 reveals that maltotriose and maltotetraose are taken up, albeit at a significantly slower rate than  
380 maltose (Fig. 3C) in *L. acidophilus* NCFM cultures. Growth experiments on two additional *L.*  
381 *acidophilus* strains confirmed that the strain possessing the transposase grew similarly poorly as *L.*

382 *acidophilus* NCFM, whereas the strain that lacks this insertion displayed better relative growth on  
383 maltotriose maltotetraose (Fig. S2).

384 Despite the weak growth, pullulanase activity was reliably measured during growth on  
385 maltotriose, maltotetraose and  $\beta$ -limit dextrin, but not on glucose (Fig. 3B). The pullulanase activity  
386 was detectable only in the cell fraction, providing evidence that the enzyme is cell attached. Thin  
387 layer chromatography analysis on samples from the pullulan assays with the cell fraction confirmed  
388 the pullulanase type debranching activity since the sole end product released was maltotriose. This  
389 precluded other enzymatic activities (*e.g.* neopullulanase or  $\alpha$ -glucosidase) being responsible for the  
390 increase in reducing sugars from pullulan degradation (Fig. S3). The only predicted extracellular  
391 pullulanase in *L. acidophilus* NCFM is LaPul13\_14 (locus tag LBA1710) (28). The inactivation of  
392 the gene encoding this enzyme abolished the cell attached pullulanase activity, providing  
393 compelling evidence that LaPul13\_14 is the sole extracellular  $\alpha$ -glucan debranching enzyme in *L.*  
394 *acidophilus* NCFM (Fig. 4).

395 The gene encoding LaPul13\_14 resides on a separate locus than the maltodextrin utilization  
396 cluster (26). The repression of pullulanase activity in the presence of glucose is suggestive of  
397 regulation through global catabolite repression (52). Indeed, this enzyme was not identified in the  
398 exoproteome of *L. acidophilus* NCFM grown on glucose in a recent proteomic analysis of S-layer  
399 associated proteins (50). A similar observation was made in a proteome analysis of *L. acidophilus*  
400 NCFM grown on raffinose, where LaPul13\_14 was repressed in the presence of glucose (53), but  
401 was clearly detectable in the presence of raffinose suggesting a level of constitutive expression of  
402 the enzyme in the absence of glucose.

403 **LaPul13\_14 confers efficient targeting of small branched  $\alpha$ -glucans.** Given the dominance of  
404 starch in human nutrition, the metabolism of this glucan by the HGM has been subject to extensive  
405 studies. *Ruminococcus bromii* has been identified as the primary degrader of resistant starch in the  
406 human gut (23), although *Bifidobacterium adolescentis* strains were also reported to possess growth  
407 capabilities on this substrate (15). Major commensals from the *Bacteroides* genus (54) and the

408 butyrate producing Firmicutes *Eubacterium rectale* (14) are other HGM with considerable starch  
409 growth and degradation capabilities. Common to these bacteria is that they possess highly modular  
410 extracellular cell-attached enzymes with one or more catalytic modules and multiple carbohydrate  
411 binding modules (CBMs), which mediate tight binding to starch substrates.

412 Only a few *Lactobacillus* strains have been demonstrated to utilize only soluble starch (18, 19,  
413 55). This is in agreement with the rare occurrence of genes encoding extracellular  $\alpha$ -glucan enzymes  
414 in this genus (1.6% or 11 out of 696 GH13 genes). Notably, only four *Lactobacillus* species encode  
415 these extracellular enzymes: *L. acidophilus*, *Lactobacillus amylovorus*, *Lactobacillus plantarum*,  
416 and *Lactobacillus manihotivorans* (Table S1). *L. plantarum* and *L. amylophilus* GV6 possess  
417 amylopullulanases (pullulanase type II) that degrade both  $\alpha$ -1,4- and  $\alpha$ -1,6-branches in starch (56–  
418 58). Notably, these starch utilizing strains stem from other ecological niches than the human gut. By  
419 contrast, *LaPul13\_14* and its homologues that display an identical domain organization, represent  
420 the main extracellular amylolytic activity in human gut lactobacilli (Table S1). This unique modular  
421 organization and the presence of the SLAP domain in gut lactobacilli, raise a question on the  
422 importance of these enzymes in the gut niche.

423 The lack of activity of *LaPul13\_14* on granular starch and the very weak binding to this substrate  
424 ( $K_d > 40 \text{ mg ml}^{-1}$ , Fig. S1) are in line with the lack of growth of *L. acidophilus* NCFM on starch. By  
425 contrast, the enzyme binds the starch mimic  $\beta$ -CD with moderate affinity (Table 2). This molecule  
426 occupies the conserved +2 substrate binding subsite in pullulanases, thus acting as a competitive  
427 inhibitor (41). Our  $\beta$ -CD inhibition kinetics data on pullulan reveal an inhibition constant  $K_i = 36$   
428  $\mu\text{M}$ , which is in the same range as the  $K_d$  obtained from surface plasmon resonance binding  
429 experiments (Table 2). More interestingly, the inhibition was not purely competitive but was of  
430 mixed nature (Fig. S4), indicative of the presence of additional  $\alpha$ -glucan surface binding sites. The  
431 glucan-binding residues in the CBM41 of the pullulanases from *Streptococcus pneumoniae* (59) are  
432 conserved in *L. acidophilus* NCFM. This makes the CBM41 a plausible candidate for the additional  
433  $\alpha$ -glucan binding in *LaPul13\_14*. A possible rationale for this additional binding in *LaPul13\_14* is

434 to increase substrate affinity by increasing the local substrate concentration in the proximity to the  
435 active site. Strikingly, the  $K_m$  of *LaPul13\_14* towards pullulan is the lowest reported for any  
436 debranching enzyme (Table S2), which attests adaptation of the substrate affinity to the competitive  
437 human gut niche. The clear preference for substrates with short branches of about two–three  
438 glucose units (Table 1) may provide a metabolic advantage for *L. acidophilus*, which is able to take-  
439 up and metabolize these substrates. Based on the kinetic parameters, the most likely substrates for  
440 *LaPul13\_14* are short branched  $\alpha$ -glucans that are generated from the action of  $\alpha$ -amylases on starch  
441 or glycogen. Given the poor digestibility of branched  $\alpha$ -glucans by human enzymes and the  
442 abundance of lactobacilli in the small intestine (16), this enzyme may act on branched oligomeric  
443 substrates from human degradation of dietary starch or glycogen (Fig. 5). Such an advantage may  
444 explain the enrichment of this debranching activity in human intestinal isolates. Taken all together,  
445 the study suggests that debranching enzyme of gut lactobacilli are evolved for efficient breakdown  
446 of short branched  $\alpha$ -glucans. The high substrate affinity may facilitate access to substrates that  
447 escape human or microbial metabolism of starch and glycogen. Further work is required to relate  
448 the *in vivo* functionality of these enzymes to gut adaptation of lactobacilli further work is required to  
449 verify this.

450

## 451 ACKNOWLEDGEMENTS

452 Alexander Holm Viborg is acknowledged for providing us with bioinformatics tools for CAZyme  
453 analyses (ahv.dk). This work was supported by a grant from the Danish Strategic Research Council,  
454 Committee of Health and Nutrition, to the project “Gene Discovery and Molecular Interactions in  
455 Prebiotics/Probiotics Systems: Focus on Carbohydrate Prebiotics”. The Danish Council for  
456 Independent Research | Natural Sciences for the an instrument grant for the SPR.

## 457 REFERENCES

- 458 1. **Lozupone CA, Stombaugh JI, Gordon JI, Jansson JK, Knight R.** 2012. Diversity,  
459 stability and resilience of the human gut microbiota. *Nature* **489**:220–230.
- 460 2. **David LA, Maurice CF, Carmody RN, Gootenberg DB, Button JE, Wolfe BE, Ling A**  
461 **V, Devlin AS, Varma Y, Fischbach MA, Biddinger SB, Dutton RJ, Turnbaugh PJ.** 2014.  
462 Diet rapidly and reproducibly alters the human gut microbiome. *Nature* **505**:559–563.
- 463 3. **Martens EC.** 2016. Fibre for the future. *Nature* **529**:158–159.
- 464 4. **Sonnenburg JL, Bäckhed F.** 2016. Diet–microbiota interactions as moderators of human  
465 metabolism. *Nature* **535**:56–64.
- 466 5. **Hur KY, Lee M-S.** 2015. Gut microbiota and metabolic disorders. *Diabetes Metab J*  
467 **39**:198–203.
- 468 6. **Flint HJ, Scott KP, Duncan SH, Louis P, Forano E.** 2012. Microbial degradation of  
469 complex carbohydrates in the gut. *Gut Microbes* **3**:289–306.
- 470 7. **Koropatkin NM, Cameron EA, Martens EC.** 2012. How glycan metabolism shapes the  
471 human gut microbiota. *Nat Rev Microbiol* **10**:323–335.
- 472 8. **Tester RF, Karkalas J, Qi X.** 2004. Starch–composition, fine structure and architecture. *J*  
473 *Cereal Sci* **39**:151–165.
- 474 9. **Møller MS, Goh YJ, Viborg AH, Andersen JM, Klaenhammer TR, Svensson B, Abou**  
475 **Hachem M.** 2014. Recent insight in  $\alpha$ -glucan metabolism in probiotic bacteria. *Biologia*  
476 (Bratisl) **69**:713–721.
- 477 10. **Blazek J, Gilbert EP.** 2010. Effect of enzymatic hydrolysis on native starch granule  
478 structure. *Biomacromolecules* **11**:3275–3289.
- 479 11. **Zhang G, Hamaker BR.** 2009. Slowly digestible starch: concept, mechanism, and proposed  
480 extended glycemic index. *Crit Rev Food Sci Nutr* **49**:852–867.

- 481 12. **Fuentes-Zaragoza E, Sánchez-Zapata E, Sendra E, Sayas E, Navarro C, Fernández-**  
482 **López J, Pérez-Alvarez JA.** 2011. Resistant starch as prebiotic: A review. *Starch - Stärke*  
483 **63**:406–415.
- 484 13. **Cockburn DW, Koropatkin NM.** 2016. Polysaccharide degradation by the intestinal  
485 microbiota and its influence on human health and disease. *J Mol Biol* **428**:3230–3252.
- 486 14. **Cockburn DW, Orlovsky NI, Foley MH, Kwiatkowski KJ, Bahr CM, Maynard M,**  
487 **Demeler B, Koropatkin NM.** 2015. Molecular details of a starch utilization pathway in the  
488 human gut symbiont *Eubacterium rectale*. *Mol Microbiol* **95**:209–230.
- 489 15. **Leitch ECM, Walker AW, Duncan SH, Holtrop G, Flint HJ.** 2007. Selective colonization  
490 of insoluble substrates by human faecal bacteria. *Environ Microbiol* **9**:667–679.
- 491 16. **Donaldson GP, Lee SM, Mazmanian SK.** 2016. Gut biogeography of the bacterial  
492 microbiota. *Nat Rev Microbiol* **14**:20–32.
- 493 17. **Bull M, Plummer S, Marchesi J, Mahenthiralingam E.** 2013. The life history of  
494 *Lactobacillus acidophilus* as a probiotic: a tale of revisionary taxonomy, misidentification  
495 and commercial success. *FEMS Microbiol Lett* **349**:77–87.
- 496 18. **Petrova P, Petrov K, Stoyancheva G.** 2013. Starch-modifying enzymes of lactic acid  
497 bacteria – structures, properties, and applications. *Starch - Stärke* **65**:34–47.
- 498 19. **Velikova P, Stoyanov A, Blagoeva G, Popova L, Petrov K, Gotcheva V, Angelov A,**  
499 **Petrova P.** 2016. Starch utilization routes in lactic acid bacteria: new insight by gene  
500 expression assay. *Starch - Stärke* **68**:1–8.
- 501 20. **Wang X, Brown IL, Khaled D, Mahoney MC, Evans AJ, Conway PL.** 2002.  
502 Manipulation of colonic bacteria and volatile fatty acid production by dietary high amylose  
503 maize (amylomaize) starch granules. *J Appl Microbiol* **93**:390–397.
- 504 21. **Le Blay GM, Michel CD, Blottière HM, Cherbut CJ.** 2003. Raw potato starch and short-  
505 chain fructo-oligosaccharides affect the composition and metabolic activity of rat intestinal

microbiota differently depending on the caecocolonic segment involved. J Appl Microbiol  
**94**:312–320.

22. **Ordiz MI, May TD, Mihindukulasuriya K, Martin J, Crowley J, Tarr PI, Ryan K, Mortimer E, Gopalsamy G, Maleta K, Mitreva M, Young G, Manary MJ.** 2015. The effect of dietary resistant starch type 2 on the microbiota and markers of gut inflammation in rural Malawi children. Microbiome **3**:1–9.

23. **Ze X, Duncan SH, Louis P, Flint HJ.** 2012. *Ruminococcus bromii* is a keystone species for the degradation of resistant starch in the human colon. ISME J **6**:1535–1543.

24. **Møller MS, Fredslund F, Majumder A, Nakai H, Poulsen J-CN, Lo Leggio L, Svensson B, Abou Hachem M.** 2012. Enzymology and structure of the GH13\_31 glucan 1,6- $\alpha$ -glucosidase that confers isomaltooligosaccharide utilization in the probiotic *Lactobacillus acidophilus* NCFM. J Bacteriol **194**:4249–4259.

25. **Andersen JM, Barrangou R, Hachem MA, Lahtinen SJ, Goh Y-J, Svensson B, Klaenhammer TR.** 2012. Transcriptional analysis of prebiotic uptake and catabolism by *Lactobacillus acidophilus* NCFM. PLoS One **7**:e44409.

26. **Nakai H, Baumann MJ, Petersen BO, Westphal Y, Schols H, Dilokpimol A, Abou Hachem M, Lahtinen SJ, Duus JØ, Svensson B.** 2009. The maltodextrin transport system and metabolism in *Lactobacillus acidophilus* NCFM and production of novel  $\alpha$ -glucosides through reverse phosphorylation by maltose phosphorylase. FEBS J **276**:7353–7365.

27. **Altermann E, Russell WM, Azcarate-Peril MA, Barrangou R, Buck BL, McAuliffe O, Souther N, Dobson A, Duong T, Callanan M, Lick S, Hamrick A, Cano R, Klaenhammer TR.** 2005. Complete genome sequence of the probiotic lactic acid bacterium *Lactobacillus acidophilus* NCFM. Proc Natl Acad Sci U S A **102**:3906–3912.

28. **Lombard V, Golaconda Ramulu H, Drula E, Coutinho PM, Henrissat B.** 2014. The carbohydrate-active enzymes database (CAZy) in 2013. Nucleic Acids Res **42**:490–495.

- 531 29. **Marchler-Bauer A, Derbyshire MK, Gonzales NR, Lu S, Chitsaz F, Geer LY, Geer RC,**  
532 **He J, Gwadz M, Hurwitz DI, Lanczycki CJ, Lu F, Marchler GH, Song JS, Thanki N,**  
533 **Wang Z, Yamashita R a., Zhang D, Zheng C, Bryant SH.** 2015. CDD: NCBI's conserved  
534 domain database. *Nucleic Acids Res* **43**:D222–D226.
- 535 30. **Bertoldo C, Antranikian A.** 2002. Starch-hydrolyzing enzymes from thermophilic archaea  
536 and bacteria. *Curr Opin Chem Biol* **6**:151–160.
- 537 31. **Domań-Pytka M, Bardowski J.** 2004. Pullulan degrading enzymes of bacterial origin. *Crit*  
538 *Rev Microbiol* **30**:107–121.
- 539 32. **Møller MS, Henriksen A, Svensson B.** 2016. Structure and function of  $\alpha$ -glucan  
540 debranching enzymes. *Cell Mol Life Sci* **73**:2619–2641.
- 541 33. **Finn RD, Cogill P, Eberhardt RY, Eddy SR, Mistry J, Mitchell AL, Potter SC, Punta**  
542 **M, Qureshi M, Sangrador-Vegas A, Salazar GA, Tate J, Bateman A.** 2016. The Pfam  
543 protein families database: towards a more sustainable future. *Nucleic Acids Res* **44**:D279–  
544 D285.
- 545 34. **Petersen TN, Brunak S, von Heijne G, Nielsen H.** 2011. SignalP 4.0: discriminating signal  
546 peptides from transmembrane regions. *Nat Methods* **8**:785–786.
- 547 35. **Kimmel SA, Roberts RF.** 1998. Development of a growth medium suitable for  
548 exopolysaccharide production by *Lactobacillus delbrueckii* ssp. *bulgaricus* RR. *Int J Food*  
549 *Microbiol* **40**:87–92.
- 550 36. **Goh YJ, Andrea Azcárate-Peril M, O'Flaherty S, Durmaz E, Valence F, Jardin J,**  
551 **Lortal S, Klaenhammer TR.** 2009. Development and application of a *upp*-based  
552 counterselective gene replacement system for the study of the S-layer protein SlpX of  
553 *Lactobacillus acidophilus* NCFM. *Appl Environ Microbiol* **75**:3093–3105.
- 554 37. **Horton RM, Hunt HD, Ho SN, Pullen JK, Pease LR.** 1989. Engineering hybrid genes  
555 without the use of restriction enzymes: gene splicing by overlap extension. *Gene* **77**:61–68.



- 556 38. **Goh YJ, Klaenhammer TR.** 2010. Functional roles of aggregation-promoting-like factor in  
557 stress tolerance and adherence of *Lactobacillus acidophilus* NCFM. Appl Environ Microbiol  
558 **76**:5005–5012.
- 559 39. **Fredslund F, Abou Hachem M, Jonsgaard Larsen R, Gerd Sørensen P, Coutinho PM,**  
560 **Lo Leggio L, Svensson B.** 2011. Crystal structure of  $\alpha$ -galactosidase from *Lactobacillus*  
561 *acidophilus* NCFM: Insight into tetramer formation and substrate binding. J Mol Biol  
562 **412**:466–480.
- 563 40. **Barkholt V, Jensen AL.** 1989. Amino acid analysis: Determination of cysteine plus half-  
564 cystine in proteins after hydrochloric acid hydrolysis with a disulfide compound as additive.  
565 Anal Biochem **177**:318–322.
- 566 41. **Vester-Christensen MB, Abou Hachem M, Naested H, Svensson B.** 2010. Secretory  
567 expression of functional barley limit dextrinase by *Pichia pastoris* using high cell-density  
568 fermentation. Protein Expr Purif **69**:112–119.
- 569 42. **Sanders ME, Klaenhammer TR.** 2001. Invited review: the scientific basis of *Lactobacillus*  
570 *acidophilus* NCFM functionality as a probiotic. J Dairy Sci **84**:319–31.
- 571 43. **O’Flaherty S, Klaenhammer TR.** 2010. The role and potential of probiotic bacteria in the  
572 gut, and the communication between gut microflora and gut/host. Int Dairy J **20**:262–268.
- 573 44. **Leyer GJ, Li S, Mubasher ME, Reifer C, Ouwehand AC.** 2009. Probiotic effects on cold  
574 and influenza-like symptom incidence and duration in children. Pediatrics **124**:e172–e179.
- 575 45. **Ringel-Kulka T, Palsson OS, Maier D, Carroll I, Galanko JA, Leyer G, Ringel Y.** 2011.  
576 Probiotic bacteria *Lactobacillus acidophilus* NCFM and *Bifidobacterium lactis* Bi-07 versus  
577 placebo for the symptoms of bloating in patients with functional bowel disorders: a double-  
578 blind study. J Clin Gastroenterol **45**:518–525.
- 579 46. **Andersen JM, Barrangou R, Abou Hachem M, Lahtinen S, Goh YJ, Svensson B,**  
580 **Klaenhammer TR.** 2011. Transcriptional and functional analysis of galactooligosaccharide

uptake by *lacS* in *Lactobacillus acidophilus*. *Proc Natl Acad Sci* **108**:17785–17790.

47. **Barrangou R, Azcarate-Peril MA, Duong T, Connors SB, Kelly RM, Klaenhammer TR.** 2006. Global analysis of carbohydrate utilization by *Lactobacillus acidophilus* using cDNA microarrays. *Proc Natl Acad Sci U S A* **103**:3816–3821.

48. **Johnson BR, Klaenhammer TR.** 2016. AcnB is an S-layer-associated  $\beta$ -N-acetylglucosaminidase and functional autolysin in *Lactobacillus acidophilus* NCFM. *Appl Environ Microbiol* **82**:5687–5697.

49. **Hynönen U, Palva A.** 2013. *Lactobacillus* surface layer proteins: structure, function and applications. *Appl Microbiol Biotechnol* **97**:5225–5243.

50. **Johnson BR, Hymes J, Sanozky-Dawes R, DeCrescenzo Henriksen E, Barrangou R, Klaenhammer TR.** 2016. Conserved S-layer-associated proteins revealed by exoproteomic survey of S-layer-forming lactobacilli. *Appl Environ Microbiol* **82**:134–145.

51. **Abbott DW, Higgins MA, Hyrnuik S, Pluvinaige B, Lammerts van Bueren A, Boraston AB.** 2010. The molecular basis of glycogen breakdown and transport in *Streptococcus pneumoniae*. *Mol Microbiol* **77**:183–199.

52. **Mahr K, Hillen W, Titgemeyer F.** 2000. Carbon catabolite repression in *Lactobacillus pentosus*: analysis of the *ccpA* region. *Appl Environ Microbiol* **66**:277–283.

53. **Celebioglu HU, Ejby M, Majumder A, Købler C, Goh YJ, Schmidt B, O’Flaherty S, Abou Hachem M, Lahtinen SJ, Jacobsen S, Klaenhammer TR, Brix S, Mølhave K, Svensson B.** 2016. Differential proteome and cellular adhesion analyses of the probiotic bacterium *Lactobacillus acidophilus* NCFM grown on raffinose – an emerging prebiotic. *Proteomics* **16**:1361–1375.

54. **Cameron EA, Maynard MA, Smith CJ, Smith TJ, Koropatkin NM, Martens EC.** 2012. Multidomain carbohydrate-binding proteins involved in *Bacteroides thetaiotaomicron* starch metabolism. *J Biol Chem* **287**:34614–34625.

- 606 55. **Lee HS, Gilliland SE, Carter S.** 2001. Amylolytic cultures of *Lactobacillus acidophilus*:  
607 potential probiotics to improve dietary starch utilization. Food Microbiol Saf **66**:338–344.
- 608 56. **Kim J-H, Sunako M, Ono H, Murooka Y, Fukusaki E, Yamashita M.** 2008.  
609 Characterization of gene encoding amylopullulanase from plant-originated lactic acid  
610 bacterium, *Lactobacillus plantarum* L137. J Biosci Bioeng **106**:449–459.
- 611 57. **Kim J-H, Sunako M, Ono H, Murooka Y, Fukusaki E, Yamashita M.** 2009.  
612 Characterization of the C-terminal truncated form of amylopullulanase from *Lactobacillus*  
613 *plantarum* L137. J Biosci Bioeng **107**:124–129.
- 614 58. **Vishnu C, Naveena BJ, Altaf M, Venkateshwar M, Reddy G.** 2006. Amylopullulanase—  
615 A novel enzyme of *L. amylophilus* GV6 in direct fermentation of starch to L(+) lactic acid.  
616 Enzyme Microb Technol **38**:545–550.
- 617 59. **Lammerts van Bueren A, Ficko-Blean E, Pluvinae B, Hehemann J-H, Higgins MA,**  
618 **Deng L, Ogunniyi AD, Stroehner UH, El Warry N, Burke RD, Czjzek M, Paton JC,**  
619 **Vocadlo DJ, Boraston AB.** 2011. The conformation and function of a multimodular  
620 glycogen-degrading pneumococcal virulence factor. Structure **19**:640–651.

621

TABLE 1. Hydrolysis kinetic parameters of *LaPul13\_14* towards oligomeric and polymeric  $\alpha$ -1,6-branched glucans at 37°C and pH 5.0.

Substrate	$K_m$	$k_{cat}$	$k_{cat} K_m^{-1}$	Normalized $k_{cat} K_m^{-1}$
	$mg\ ml^{-1}$	$s^{-1}$	$ml\ s^{-1}\ mg^{-1}$	
Pullulan	0.05±0.004	518±10.5	10368	100
Amylopectin	0.37±0.041	25±0.7	67	0.6
$\beta$ -limit dextrin	0.20±0.090	189±15.8	945	9
6 <sup>2</sup> - $\alpha$ -D-maltosyl maltotriose	0.33±0.040 <sup>a</sup>	378±18.0 <sup>b</sup>	1145 <sup>c</sup>	

<sup>a</sup> mM; <sup>b</sup> s<sup>-1</sup>; <sup>c</sup> mM<sup>-1</sup> s<sup>-1</sup>

TABLE 1. Binding of cyclodextrins to *LaPul13\_14* determined by surface plasmon resonance.

Cyclic Ligand	pH	Temperature (°C)	$K_D$ ( $\mu$ M)
$\alpha$ -CD	5.0	25	89.0
$\gamma$ -CD	5.0	25	11.2
$\beta$ -CD	5.0	25	10.8
$\beta$ -CD	5.0	15	7.2
$\beta$ -CD	5.0	37	29.9
$\beta$ -CD	7.0	25	21.8

624

## 625 FIGURES

626 **FIG 1** Domain organization of *LaPul13\_14*. The abbreviations are: SP, signal peptide; CBM41,  
627 starch binding module of CBM41 in the CAZy database; N-dom, N-terminal domain of unknown  
628 function; CBM48, starch binding module of CBM48; GH13\_14, catalytic module assigned into  
629 glycoside hydrolase family 13 subfamily 14; C-terminal domain conserved in pullulanases of  
630 GH13; SLAP, surface layer association protein domain.

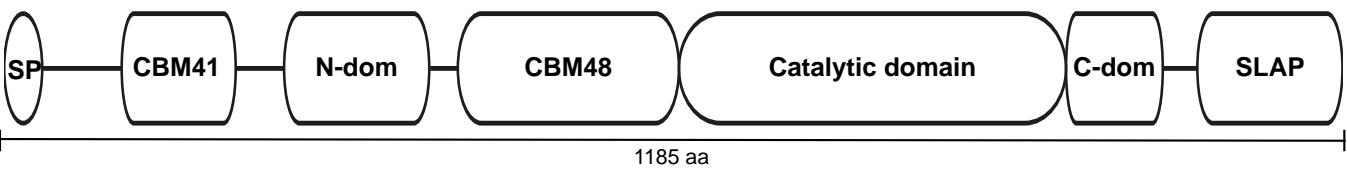
631 **FIG 2** Schematic overview of  $\alpha$ -glucans included in the present study.  $\alpha$ -1,4-linked glucose units  
632 are shown as linear hexagons and  $\alpha$ -1,6-linkages are depicted as horizontal short segments between  
633 the glucosyl unit hexagons with the reducing end depicted as a white hexagon. The small branched  
634  $\alpha$ -limit dextrin is resembling the one used in this study.  $\beta$ -Limit dextrin, produced from  $\beta$ -amylase  
635 hydrolysis of amylopectin is used to provide experimental evidence for the preference of the  
636 *LaPul13\_14* to short branches compared to amylopectin.

637 **FIG 3** (A) Growth of *L. acidophilus* NCFM on different  $\alpha$ -glucans and (B) the relative cell-  
638 associated pullulan hydrolyzing activity of *L. acidophilus* NCFM cells harvested after 10 h of  
639 growth on the  $\alpha$ -glucans shown in (A). (C) Growth of *L. acidophilus* NCFM on a total of 0.5%  
640 (w/v) mixture of maltose, maltotriose, and maltotetraose (1:1:1 based on weight), and its utilization  
641 of the substrates was analysed by HPAEC-PAD. Only the debranched mainly maltose and  
642 maltotriose are used from  $\beta$ -Limit dextrin during growth on this substrate, which explains the much  
643 lower degree of growth per mass substrate as compared to maltose.

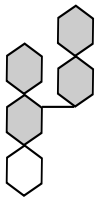
644 **FIG 4** (A) Comparison of the growth of wildtype *L. acidophilus* NCFM and the *LaPul13\_14* gene  
645 deletion strain ( $\Delta$ LBA1710) on glucose or maltose, and (B) the cell-associated pullulan hydrolyzing  
646 activity of cells harvested after 10 h of growth.

647 **FIG 5** Schematic overview of the extracellular  $\alpha$ -glucan metabolism of *L. acidophilus* NCFM. The  
648 cell-attached pullulanase activity of *LaPul13\_14* mediates the debranching of preferentially smaller  
649 branched oligomers that possibly are products from human or bacterial degradation of amylopectin,  
650 which is signified by a dashed line. The produced maltose and short maltooligosaccharides are

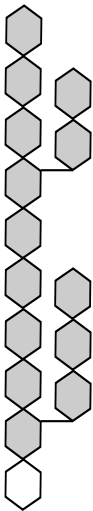
651 taken up by one or more specific transporters and degraded intracellularly by the enzymes encoded  
652 by the maltooligosaccharide utilization locus to produce  $\beta$ -glucose-1-phosphate and glucose, which  
653 enter glycolysis (26).



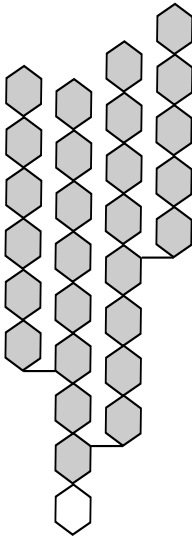




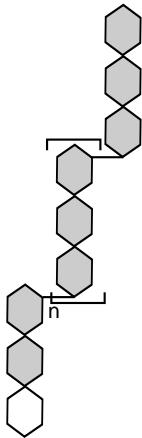
Small branched  
 $\alpha$ -limit dextrin



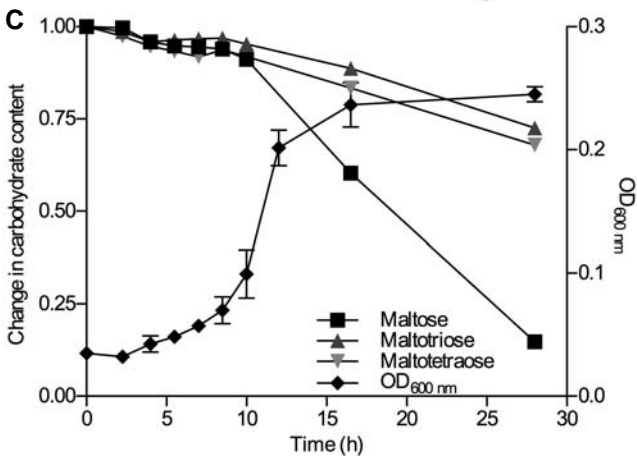
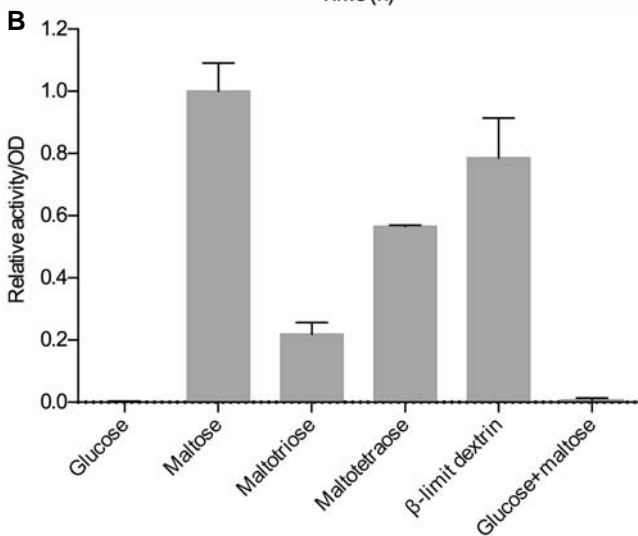
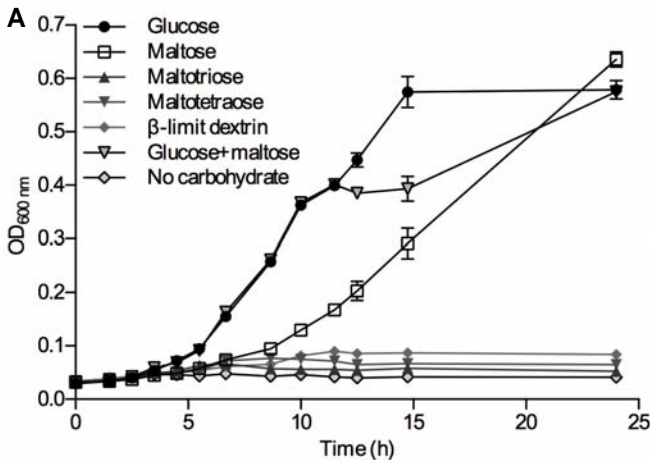
$\beta$ -limit dextrin

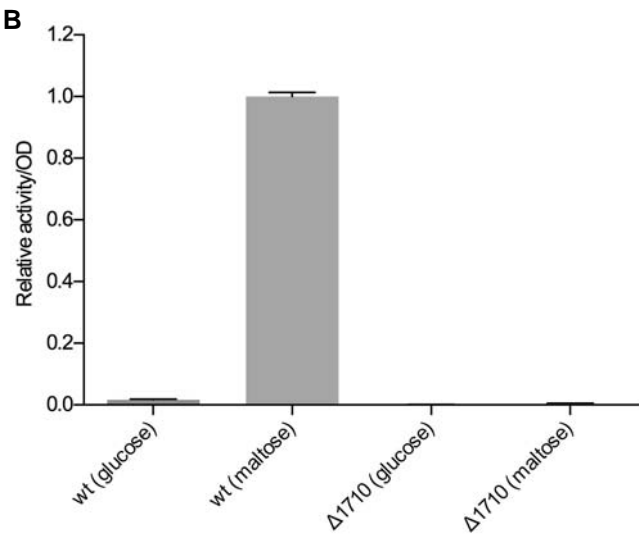
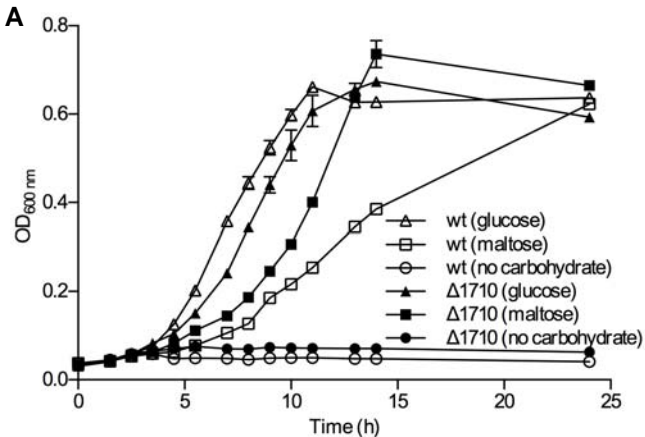


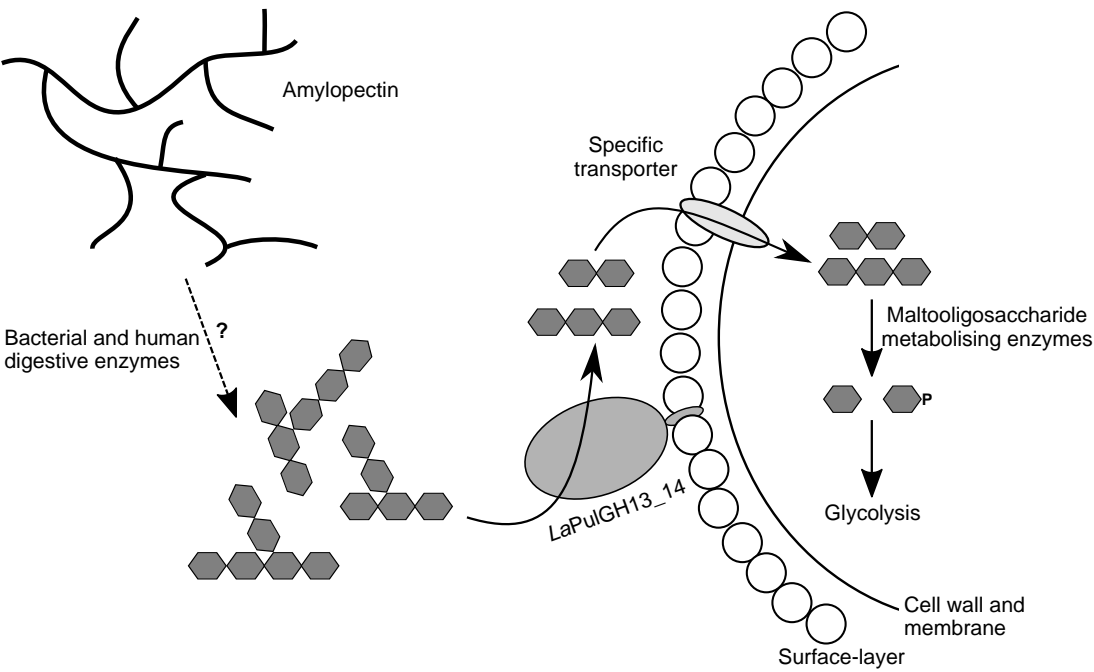
Amylopectin



Pullulan







## SUPPLEMENTAL MATERIAL

### **An extracellular cell-attached pullulanase confers branched $\alpha$ -glucan utilization in the human gut probiotic *Lactobacillus acidophilus* NCFM**

Marie S. Møller,<sup>a</sup> Yong Jun Goh,<sup>b</sup> Kasper Bøwig Rasmussen,<sup>a\*</sup> Wojciech Cypryk,<sup>a\*</sup> Hasan Ufuk Celebioglu,<sup>a</sup> Todd R. Klaenhammer,<sup>b</sup> Birte Svensson,<sup>a</sup> Maher Abou Hachem<sup>a#</sup>

Department of Biotechnology and Biomedicine, Technical University of Denmark, Kgs. Lyngby, Denmark<sup>a</sup>;  
Department of Food, Bioprocessing and Nutrition Sciences, North Carolina State University, Raleigh, North Carolina<sup>b</sup>

#Address correspondence to Maher Abou Hachem, [maha@bio.dtu.dk](mailto:maha@bio.dtu.dk) and Yong Jun Goh [yjgoh@ncsu.edu](mailto:yjgoh@ncsu.edu).

\*Present address: Kasper Bøwig Rasmussen, Novo Nordisk A/S, Gentofte, Denmark; Wojciech Cypryk, Department of Bioorganic Chemistry, Polish Academy of Sciences, Lodz, Poland.

**Table S1.** Predicted extracellular enzymes (SignalP (1)) of GH13 from available *Lactobacillus* genomes.

Genbank accession	Organism	GH13 subfamily <sup>a</sup>	SLAP domain <sup>b</sup>	Isolate origin
AAV43522	<i>L. acidophilus</i> NCFM	14	+	<b>Human gut</b>
AJP47013	<i>L. acidophilus</i> FSI4	14	+	Yogurt
AGK94861	<i>L. acidophilus</i> La-14	14	+	<b>Human gut</b>
ADZ06675	<i>L. amylovorus</i> 30SC	14	+	<b>Porcine gut</b>
ADQ58495	<i>L. amylovorus</i> GRL1112	14	+	<b>Porcine gut</b>
AEA31469	<i>L. amylovorus</i> GRL1118	14	+	<b>Porcine ileum</b>
AAC45781	<i>L. amylovorus</i> CIP 102989	28	-	Cattle (waste-corn fermentation)
AAD45245	<i>L. manihotivorus</i> LMG 18010T	28	-	Cassava
AAC45780	<i>L. plantarum</i> A6	28	-	Cassava
BAF93906	<i>L. plantarum</i> L137	14	-	Fermented food
AHX97726	<i>L. plantarum</i> S21	28	-	Fermented rice noodles

<sup>a</sup>Subfamily classification in the CAZy data base (www.CAZy.org).

<sup>b</sup>The occurrence of a surface layer association protein domain in the enzyme is denoted by “+”

**Table S2.** Comparison of kinetic parameters of pullulanases. Purple, GH13\_13, i.e. enzymes mainly acting on  $\beta$ -limit dextrins; Blue, GH13\_14, i.e. enzymes with activity on  $\beta$ -limit dextrins as well as the polymeric  $\alpha$ -glucans amylopectin and glycogen; Orange, Unclassified/no protein sequence in CAZy. The enzyme from *L. acidophilus* NCFM displays the highest catalytic efficiency for any debranching enzyme owing to an unprecedented low  $K_m$ .

Organism	pH, temperature	$K_m$ $mg\ ml^{-1}$	$k_{cat}$ $s^{-1}$	$k_{cat}/K_m$ $ml\ s^{-1}\ mg^{-1}$	Reference
<b>PULLULAN</b>					
Barley ( <i>Hordeum vulgare</i> )	5.5, 37°C	0.081±0.003	61±13	753	(2)
<i>Klebsiella pneumoniae</i> ,	5.0, 40°C	0.017	103.3	6076	(3)
<i>Klebsiella pneumoniae</i>	5.4, 37°C	0.617	116	188	(4)
Rice ( <i>Oryza sativa</i> L. <i>japonica</i> )	6.0, 37°C	0.625	23.1	37.0	(5)
Spinach ( <i>Spinacia oleracea</i> )	6.0, 37°C	0.78/0.70			(6, 7)
<i>Anaerobranca gottschalkii</i>	8, 60°C	0.75			(8)
<i>Bacillus acidopullulyticus</i>	5.0, 70°C	4.0			(9)
<i>Bacillus deramificans</i>	4.5, 60°C	0.70±0.02	1900.4±103.5	2712.9±121.6	(10)
<i>Bacillus subtilis</i> strain 168	5.4, 37°C	1.284	97	75.5	(4)
<i>Exiguobacterium</i> sp. SH3	7.0, 37°C	0.069			(11)
<i>Fervidobacterium pennavorans</i>	6.0, 80°C	0.4			(12)
<b><u><i>Lactobacillus acidophilus</i> NCFM</u></b>	<b><u>5.0, 37°C</u></b>	<b><u>0.05±0.004</u></b>	<b><u>518.4±10.5</u></b>	<b><u>10368</u></b>	<b><u>This study</u></b>
<i>Paenibacillus barengoltzi</i>	5.5, 50°C	2.94			(13)
<i>Paenibacillus polymyxa</i> Nws-pp2	6.0, 35°C	15.25			(14)
<i>Bacillus cereus</i> Nws-bc5	7.0, 40°C	0.45			(15)
<i>Bacillus megaterium</i> WW1210	6.5, 55°C	3.3±0.25			(16)
<i>Bacillus naganoensis</i>	4.5, 60°C	1.22±0.11	0.72±0.01	0.59	(17)
<i>Bacillus</i> sp. AN-7	6, 80°C	1.3			(18)
<i>Bacillus</i> sp. S-1	9.0, 50°C	7.92			(19)
<i>Thermoanaerobacter thermohydrosulfuricus</i> ( <i>Clostridium thermohydrosulfuricum</i> )	6.0, 60°C	0.675	271	410	(20)
<i>Exiguobacterium acetylium</i> a1/YH5	6.0, 50°C	0.12±0.02			(21)
<i>Lactococcus lactis</i> IBB 500	4.5, 60°C	0.34±0.02			(22)
Oat ( <i>Avena sativa</i> )	5.0, 30°C	0.17			(23)
<i>Sorghum bicolor</i>	5.0, 30°C	0.2			(24)
Sugar beet ( <i>Beta vulgaris</i> var. <i>altissima</i> )	5.6, 37°C	0.31			(25)
<i>Thermus caldophilus</i> GK-24	7.0, 73°C	0.42			(26)
<b>POTATO AMYLOPECTIN</b>					
Barley ( <i>Hordeum vulgare</i> )	5.5, 37°C	6.9±1.0	15.6±1.2	2.3	(27)
<i>Klebsiella pneumoniae</i>	5.5, 40°C	10.1	14.1		(3)
Rice ( <i>Oryza sativa</i> L. <i>japonica</i> )	6.0, 37°C	1.538			(5)
Spinach ( <i>Spinacia oleracea</i> )	6.0, 37°C	7			(6, 7)
<b><u><i>Lactobacillus acidophilus</i> NCFM</u></b>	<b><u>5.0, 37°C</u></b>	<b><u>0.37±0.041</u></b>	<b><u>24.9±0.7</u></b>	<b><u>67</u></b>	<b><u>This study</u></b>
<i>Bacillus megaterium</i> WW1210	6.5, 55°C	3.6±0.18			(16)
<i>Bacillus</i> sp. S-1	9.0, 50°C	1.63			(19)
Broad bean ( <i>Vicia faba</i> L.)	30°C	1.2			(28)
Oat ( <i>Avena sativa</i> )	5.0, 30°C	1.4			(23)
Sugar beet ( <i>Beta vulgaris</i> var. <i>altissima</i> )	5.6, 37°C	4.55			(25)
<b>AMYLOPECTIN <math>\beta</math>-LIMIT DEXTRIN</b>					
Broad bean ( <i>Vicia faba</i> L.)	30°C	1			(28)
<i>Sorghum bicolor</i>	5.0, 37°C	2.5			(24)
<b><u><i>Lactobacillus acidophilus</i> NCFM</u></b>	<b><u>5.0, 37°C</u></b>	<b><u>0.20±0.090</u></b>	<b><u>189±15.8</u></b>	<b><u>945</u></b>	<b><u>This study</u></b>

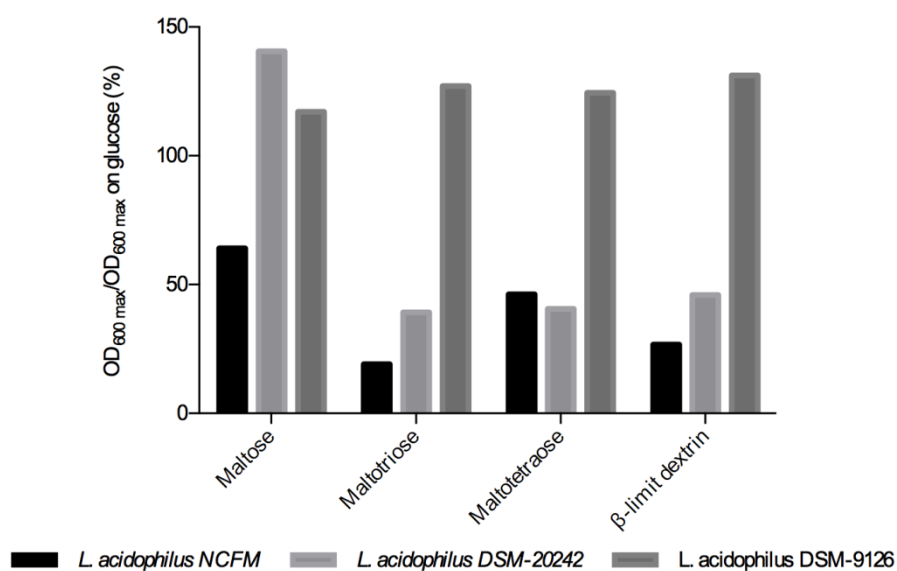


**Fig. S1.** Maximal growth of three *L. acidophilus* strains on maltooligosaccharides and  $\beta$ -limit dextrin relative to the maximal growth on glucose. *L. acidophilus* NCFM and *L. acidophilus* DSM-20242 have a comparable maltooligosaccharides utilisation gene cluster, *i.e.* they have a transposase included in the cluster. The *L. acidophilus* DSM-9126 does not have a transposase in its maltooligosaccharides utilisation gene cluster, and is likely to have an intact expression of the ATP-binding cassette transporter.



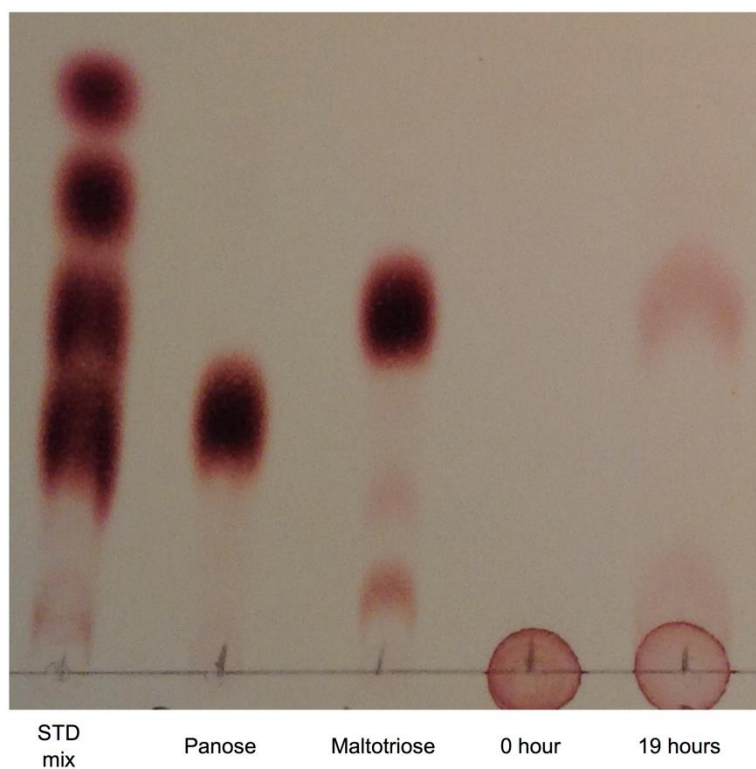


**Fig. S2.** Thin layer chromatography analysis of the degradation product from whole cell assay with pullulan. The standard mix (STD mix) consists of 20 mM of (mentioned from the top); glucose, maltose, maltotriose, panose. Furthermore, 20 mM panose and 20 mM maltotriose were spotted separately. The plate clearly shows the exclusive release of maltotriose after 19 h (first lane on the right side of the plate), confirming the pullulanase activity.

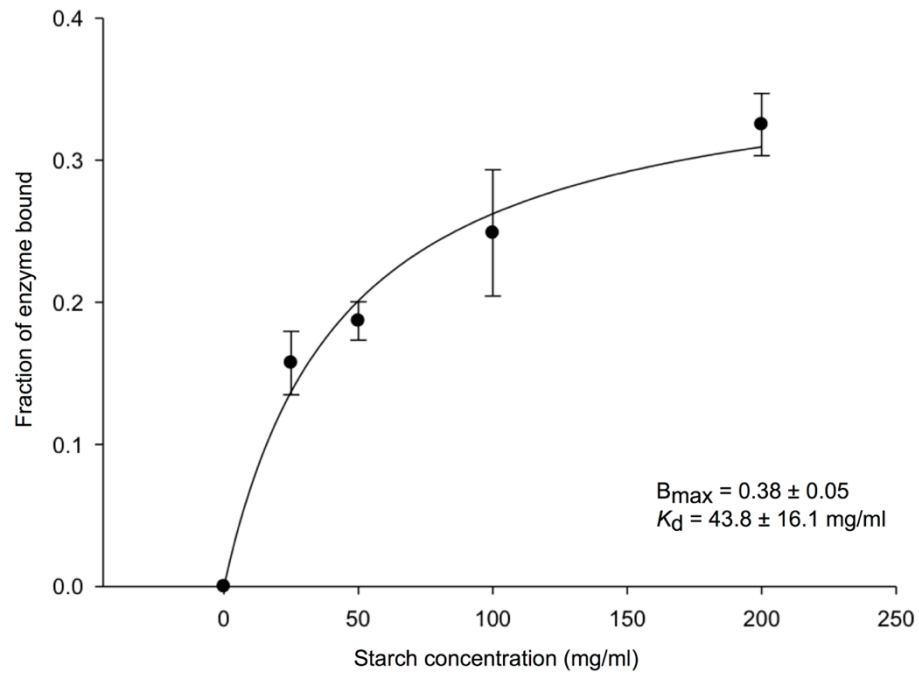


**Fig. S3.** Binding of *LaPul13\_14* to starch granules. The data is from four replicate experiments. The solid line is the fit of a one binding site model to the data, with the  $B_{\max}$  and the  $K_d$  as the maximum binding capacity and dissociation constant, respectively.

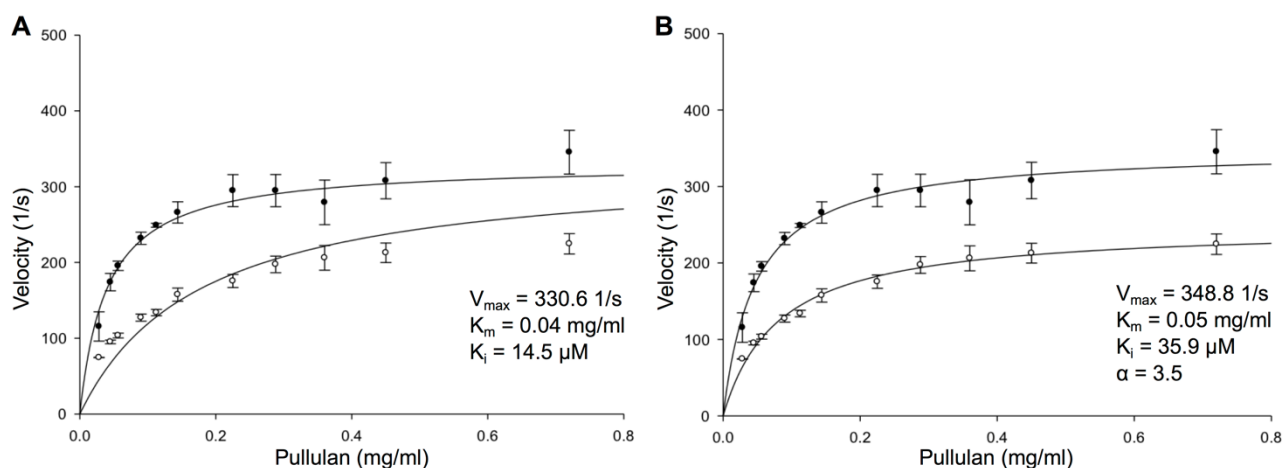


**Fig. S4.** Inhibition kinetics of *LaPul13\_14* on pullulan by  $\beta$ -cyclodextrin (50  $\mu\text{M}$ ). Two different inhibition models are shown. The solid and hollow circles represent the initial rates in the absence and the presence of  $\beta$ -cyclodextrin, respectively. The solid lines represent the fit to: (A) a competitive inhibition model and (B) mixed inhibition model. The competitive inhibition model results in systematic poor fits to the data, whereas the data is well modelled by a mixed inhibition model, which is the best model also as compared to a non-competitive inhibition model (not shown).

## REFERENCES:

1. **Petersen TN, Brunak S, von Heijne G, Nielsen H.** 2011. SignalP 4.0: discriminating signal peptides from transmembrane regions. *Nat Methods* **8**:785–786.
2. **Vester-Christensen MB, Abou Hachem M, Naested H, Svensson B.** 2010. Secretory expression of functional barley limit dextrinase by *Pichia pastoris* using high cell-density fermentation. *Protein Expr Purif* **69**:112–119.
3. **Yokobayashi K, Akai H, Sugimoto T, Hirao M, Sugimoto K, Harada T.** 1973. Comparison of the kinetic parameters of *Pseudomonas* isoamylase and *Aerobacter* pullulanase. *Biochim Biophys Acta* **293**:197–202.
4. **Malle D, Itoh T, Hashimoto W, Murata K, Utsumi S, Mikami B.** 2006. Overexpression, purification and preliminary X-ray analysis of pullulanase from *Bacillus subtilis* strain 168. *Acta Crystallogr Sect F Struct Biol Cryst Commun* **62**:381–384.
5. **Yamasaki Y, Nakashima S, Konno H.** 2008. Pullulanase from rice endosperm. *Acta Biochim Pol* **55**:507–510.
6. **Ludwig I, Ziegler P, Beck E.** 1984. Purification and properties of spinach leaf debranching enzyme. *Plant Physiol* **74**:856–861.
7. **Renz A, Schikora S, Schmid R, Kossmann J, Beck E.** 1998. cDNA sequence and heterologous expression of monomeric spinach pullulanase: multiple isomeric forms arise from the same polypeptide. *Biochem J* **331**:937–945.
8. **Bertoldo C, Armbrecht M, Becker F, Scha T, Antranikian G, Liebl W.** 2004. Cloning, sequencing, and characterization of a heat- and alkali-stable type I pullulanase from *Anaerobaculum gottschalkii*. *Appl Environ Microbiol* **70**:3407–3416.
9. **Singh RS, Saini GK, Kennedy JF.** 2010. Maltotriose syrup preparation from pullulan using pullulanase. *Carbohydr Polym* **80**:401–407.
10. **Duan X, Chen J, Wu J.** 2013. Improving the thermostability and catalytic efficiency of *Bacillus deramificans* pullulanase by site-directed mutagenesis. *Appl Environ Microbiol* **79**:4072–4077.
11. **Rajaei S, Heidari R, Zahiri HS, Sharifzadeh S, Torktaf I, Noghabi KA.** 2014. A novel cold-adapted pullulanase from *Exiguobacterium* sp. SH3: Production optimization, purification, and characterization. *Starch - Stärke* **66**:225–234.
12. **Bertoldo C, Duffner F, Jorgensen PL, Antranikian G.** 1999. Pullulanase type I from *Fervidobacterium pennavorans* Ven5: cloning, sequencing, and expression of the gene and biochemical characterization of the recombinant enzyme. *Appl Environ Microbiol* **65**:2084–2091.
13. **Liu J, Liu Y, Yan F, Jiang Z, Yang S, Yan Q.** 2016. Gene cloning, functional expression and characterisation of a novel type I pullulanase from *Paenibacillus barengoltzii* and its application in resistant starch production. *Protein Expr Purif* **121**:22–30.
14. **Wei W, Ma J, Chen S-Q, Cai X-H, Wei D-Z.** 2015. A novel cold-adapted type I pullulanase of *Paenibacillus polymyxa* Nws-pp2: in vivo functional expression and biochemical characterization of glucans hydrolyzates analysis. *BMC Biotechnol* **15**:1–13.
15. **Wei W, Ma J, Guo S, Wei DZ.** 2014. A type I pullulanase of *Bacillus cereus* Nws-bc5 screening from

stinky tofu brine: Functional expression in *Escherichia coli* and *Bacillus subtilis* and enzyme characterization. *Process Biochem* **49**:1893–1902.

16. **Yang S, Yan Q, Bao Q, Liu J, Jiang Z.** 2016. Expression and biochemical characterization of a novel type I pullulanase from *Bacillus megaterium*. *Biotechnol Lett*.
17. **Chang M, Chu X, Lv J, Li Q, Tian J, Wu N.** 2016. Improving the thermostability of acidic pullulanase from *Bacillus naganoensis* by rational design. *PLoS One* **11**:e0165006.
18. **Kunamneni A, Singh S.** 2006. Improved high thermal stability of pullulanase from a newly isolated thermophilic *Bacillus* sp. AN-7. *Enzyme Microb Technol* **39**:1399–1404.
19. **Kim C-H, Choi H-I, Lee D-S.** 1993. Purification and biochemical properties of an alkaline pullulanase from alkalophilic *Bacillus* sp. S-1. *Biosci Biotechnol Biochem* **57**:1632–1637.
20. **Saha BC, Mathupala SP, Zeikus JG.** 1988. Purification and characterization of a highly thermostable novel pullulanase from *Clostridium thermohydrosulfuricum*. *Biochem J* **252**:343–348.
21. **Qiao Y, Peng Q, Yan J, Wang H, Ding H, Shi B.** 2015. Gene cloning and enzymatic characterization of alkali-tolerant type I pullulanase from *Exiguobacterium acetylicum*. *Lett Appl Microbiol* **60**:52–59.
22. **Waśko A, Polak-Berecka M, Targonski Z.** 2011. Purification and characterization of pullulanase from *Lactococcus lactis*. *Prep Biochem Biotechnol* **41**:252–261.
23. **Dunn G, Manners DJ.** 1975. The limit dextrinases from ungerminated oats (*Avena sativa* L) and ungerminated rice (*Oryza sativa* L). *Carbohydr Res* **39**:283–293.
24. **Hardie DG, Manners DJ, Yellowlees D.** 1976. The limit dextrinase from malted sorghum (*Sorghum vulgare*). *Enzyme* **50**:75–85.
25. **Masuda H, Takahashi T, Sugawara S.** 1987. Purification and properties of starch hydrolyzing enzymes in mature roots of sugar beets. *Plant Physiol* **84**:361–365.
26. **Kim CH, Nashiru O, Ko JH.** 1996. Purification and biochemical characterization of pullulanase type I from *Thermus caldophilus* GK-24. *FEMS Microbiol Lett* **138**:147–152.
27. **Møller MS, Windahl MS, Sim L, Bøjstrup M, Abou Hachem M, Hindsgaul O, Palcic M, Svensson B, Henriksen A.** 2015. Oligosaccharide and substrate binding in the starch debranching enzyme barley limit dextrinase. *J Mol Biol* **427**:1263–1277.
28. **Gordon RW, Manners DJ, Stark JR.** 1975. The limit dextrinase of the broad bean (*Vicia faba* L). *Carbohydr Res* **42**:125–134.